Lasers in Manufacturing Conference 2015

Fabrication of micro-pump device with mixing functionality in fused silica with ultrashort laser pulses

Valdemar Stankevič[a], Gediminas Račiukaitis[b]

[a]*Center for Physical Sciences and Technology, Savanoriu Ave. 231, LT-02300, Vilnius, Lithuania*
[b]*ELAS, Ltd, Savanoriu Ave. 231, LT-02300, Vilnius, Lithuania, valdemar.s@e-lasers.com*

Abstract

The microfluidic micro-pump device fabricated by femtosecond direct laser writing technique in combination with chemical etching is presented. The contour and lines scanning method was used to adjust the best etching rate of micro-pump structure inside bulk fused silica. The working principle of micro-pump is based on the Venturi tube model. The design modelling was performed using COMSOL Multiphysics. The flow dynamics inside micro-channels was investigated in order to achieve the suction effect in micro-pump. Depending on the used input flow speed, the liquid injection or pumping can be achieved. When the both inlets of the designed micro-pump were connected to liquids with different concentration of dyes, the micro-pump acted as a micro-mixer. Pumping and mixing capability of the device were characterized, depending on the input flow rate, and the results are presented.

Keywords: Microfluidic; femtosecond; transparent materials; chemical etching

1. Introduction

In microfluidics, liquids are transported through microchannels, and the main functional components are the micro-pumps and micro-mixers that can be used in active microfluidic devices referenced by *Whitesides, 2006 and Sackmann et al., 2014.* Using these components, the fully functional device can be miniaturized and embedded in a single chip. The syringe pumps are one of the most used devices for controlling the flow in microfluidic. The drawback of these pumps is that they are expensive and it is difficult to miniaturize them (*Pennathur and al., 2008)*. Miniaturization is critical for use of pumps in microfluidics. Therefore, there is a need for simple methods for creating flow in a microfluidic device. Many pumps have been developed for microfluidics that can be divided into mechanical pumps such as membrane pump (*Zengerle and al, 1995* and *Benard et al., 1997*), rotary pump (*Ahn et al., 1995*), and non-mechanical pumps: electroosmotic/electrophoretic pump (*Manz et al., 1995*). The mechanical pumps have higher pumping velocity but also moving parts. Sensitivity to particle contamination in a fluid makes it difficult to use in microfluidics as may result in a short

lifetime and low reliability. Fabrication of non-mechanical pumps is simpler but small pumping velocity and charged fluid requirement limits their application.

Conventionally, the microfluidic devices are fabricated by a combination of photolithography and chemical etching (*Madou, 2002*) or using soft lithography but these techniques can be extended only for two-dimensional patterns on the surface. To create the 3D structure, several layers need to be processed and bonded together which complicates the production. Avoiding these limitations, the femtosecond laser induced chemical etching technique (FLICE) (*Hnatovsky et al., 2006*) is an attractive solution for embed 3D microstructures in transparent materials (*Gattass et al., 2008* and *Sugioka et al., 2014*). During the past decades, the femtosecond lasers become a unique tool for 3D structures fabrication in different optical materials where the transparent materials plays crucial role due the ability of confined internal modifications and selective modified zone removing by chemical etching (*Bellouard et al., 2004* and , *Marcinkevicius et al., 2001*).

In this work, we demonstrate the novel micro-pump device based on the Venturi tube (figure 1) fabricated in fused silica by FLICE technique. The Venturi micro pump is easy to miniaturization and has no mechanical moving parts that simplify the fabrication. It is shown the ability of fluid pumping and mixing in a single device that can be attractive in different microfluidic fields. A preliminary study was performed to measure the required negative pressure for suction.

2. Design and working principle simulation

2.1. Simulation of fluid flow

The Venturi tube *(Koo et al., 2006)* produces pressure drop without moving parts in vena contracta region and consists of a converging and diverging channels with an additional pumping channel. The liquid enters the device with a cross section area S_{in}, pressure P_{in} and velocity v_{in}. According the fluid continuity the volumetric flow rate at vena contracta should be maintained constant that means that fluid velocity in throat will be faster and that can be derived from Bernoulli's principle and continuity equation:

$$P_{in} - P_t = \frac{\rho}{2}(v_t^2 - v_{in}^2) = \frac{\rho}{2} v_{in}^2 \left(\frac{S_{in}^2}{S_t^2} - 1 \right) \qquad (1)$$

where P_{in}, P_t are inlet and throat pressures, ρ is density, v_{in}, v_t are inlet and throat velocities, and S_{in}, S_t are the channel cross-section areas.

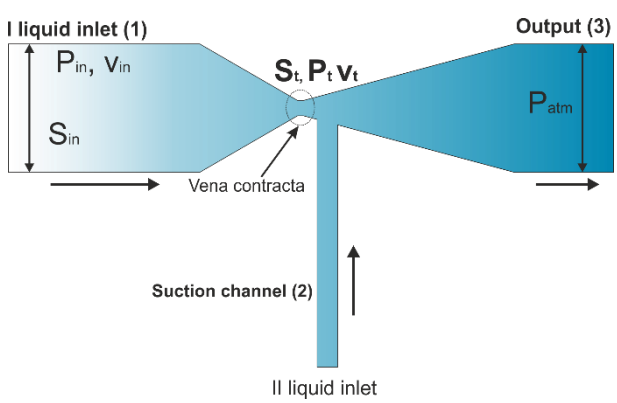

1 Fig. Schematic drawing of the Venturi based micro-pump. The outlet is open to the atmosphere.

The accelerated liquid in the vena contracta region creates a pressure drop which should be compensated by the negative pressure and a suction flow from inlet II appears. The design of the micro-pump device was adjusted to maximize the negative pressure. The Comsol Multiphysics software was used to optimize the micro-pump design and to find the threshold velocity to initiate the suction. The Navier-Stokes equation for laminar flow was solved:

$$\rho(\frac{\partial u}{\partial t} + u \cdot \nabla u) = \left[-\nabla p + \mu \nabla^2 u\right] + F \qquad (2)$$

where ρ is the liquid density, **v** is the velocity vector, p is the pressure, μ is the dynamic viscosity and F is the gravity force. The main assumptions that were made during modelling is: no-slip boundary condition and steady-state laminar flow condition. The simulation results are shown in figure 2. As the fluid used for micro-pump characterization was water, the table 1 shows the main water parameters used in the simulation.

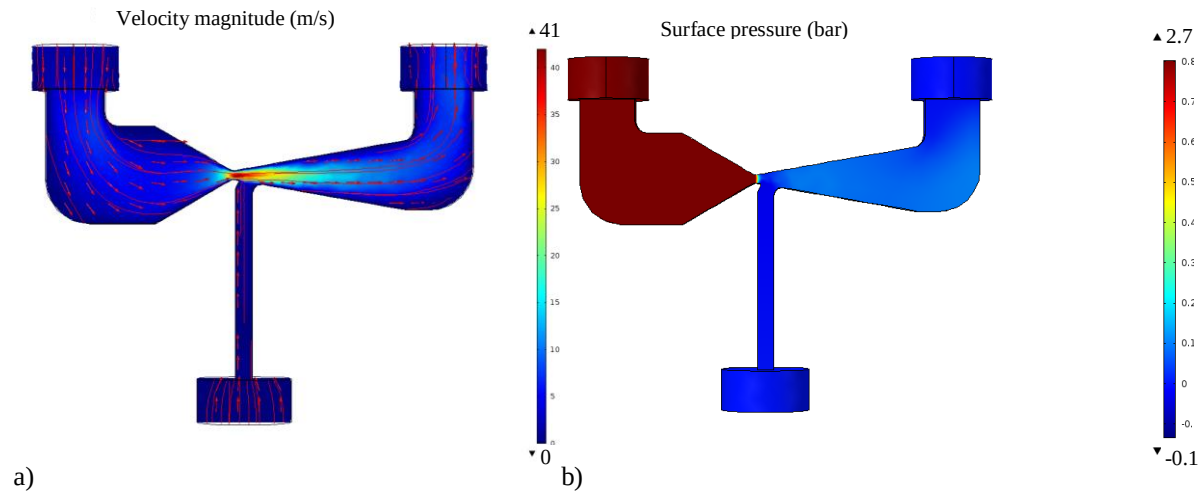

Fig 2 The velocity distribution (a) and pressure field (b) when the inlet water velocity is 1 m/s. The negative pressure in the vena contracta is -0.05 bar.

1 Table. The fluid parameters used in the simulation.

Parameter	*Value*	*Unit*
Density	1000	kg/m^3
Viscosity	0.001	Pa·s
Diffusion coefficient	2.99e-9	m^2/s
Inlet fluid velocity	0.1-2	m/s
Concentration	1	mol/mm^3

2.2. Simulation of mixing capacity

To describe the diffusive transport a Fick's law can be used. At the macroscopic level, systems usually mix fluids using mechanical actuators or turbulent 3D flow. At the micro-scale level, however, neither of these

approaches is practical or even possible. Inside the mixer, the following convection-diffusion equation describes the concentration of the dissolved substances in a fluid:

$$\frac{\partial c}{\partial t} + \nabla \cdot (-D \nabla c) = R - u \cdot \nabla c \qquad (3)$$

where c is the concentration, D is the diffusion coefficient, and R is the reaction rate. In this model, $D = 2.99 \cdot 10^{-9}$ m^2/s and $R = 0$, because the concentration is not affected by any reaction. The mixing results when the inlet concentration was 1 mol/mm^3 and the concentration in the suction channel was 0 mol/mm^3, and vice versa are shown in the figure 3.100 kHz

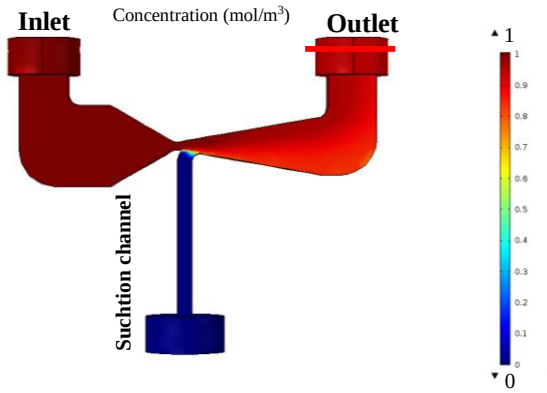

a)

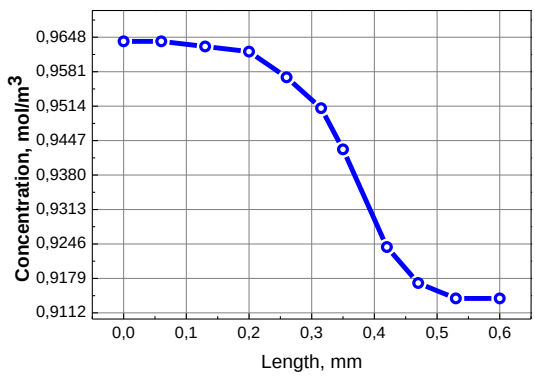

b)

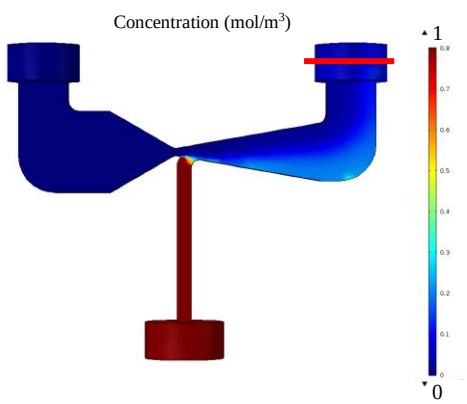

c)

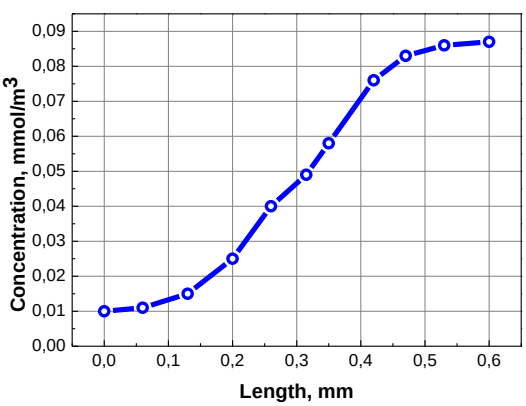

d)

Fig. 3 The ink concentration distribution in micro-pump device after 1s: (a) Ink concentration at inlet is 1mol/m^3 and at suction channel ink concentration is 0 mol/m^3; (b) Ink concentration distribution at the cross section of the outlet micro-channel (at indicated red line); (c) Ink concentration at inlet is 0 mol/m^3 and at suction channel ink concentration is 1 mol/m^3; (d) Ink concentration distribution at the cross section of the outlet micro-channel (indicated red line).

According to the simulation results, it is evident that the concentration distribution at the output of the micro-pump is not uniform. The difference between minimal and maximal concentration is ~ 10 %. In the case when 1 mol/mm^3 concentration of ink is at the inlet (fig 3 a), the concentration gradient at the outlet is positive and opposite gradient value when the concentration of 1 mol/mm^3 goes from the suction channel (fig 3 c).

3. Fabrication of micro-pump device

The micro-suction device was fabricated by direct laser writing technique. The femtosecond Yb:KGW laser beam with 300 fs pulse duration, 500 kHz repetition rate, and 400 nJ pulse energy was directed to the commercially available 15x4x2 mm^3 fused silica sample (JGS1). The beam was focused by the 50x (NA = 0.55) objective at a depth of ~ 550 µm below the sample surface. Tthe sample was moved perpendicularly to the beam propagation direction by a precision translation stage at a speed of ~ 3 mm/s. The 3D micro-pump device was sliced to virtual vertical planes, and each plane was fabricated by the contour scanning method (*Stankevič et al., 2014*). The linear polarization was set perpendicular to the x-axis direction. The modified sample was immersed in diluted 15 % HF acid for ~ 15 hours subsequent etching at 30 ºC temperature without ultrasonic batch. Fabricated micro-suction device possessed the micro-channels with a rectangular cross section. The inlet cross section was ~ 670x150 µm^2; the vena contracta cross section was ~ 63x150 µm^2 and the outlet cross section was ~ 455x150 µm^2. The cross section of the suction channel was ~ 122x150 µm^2. During the experiments, a few designs of micro-pumps were fabricated (figure 4). The micro-pump of the first design was fabricated without the simulation approach and exhibited no suction effect, the second and third design versions were optimized during the simulation.

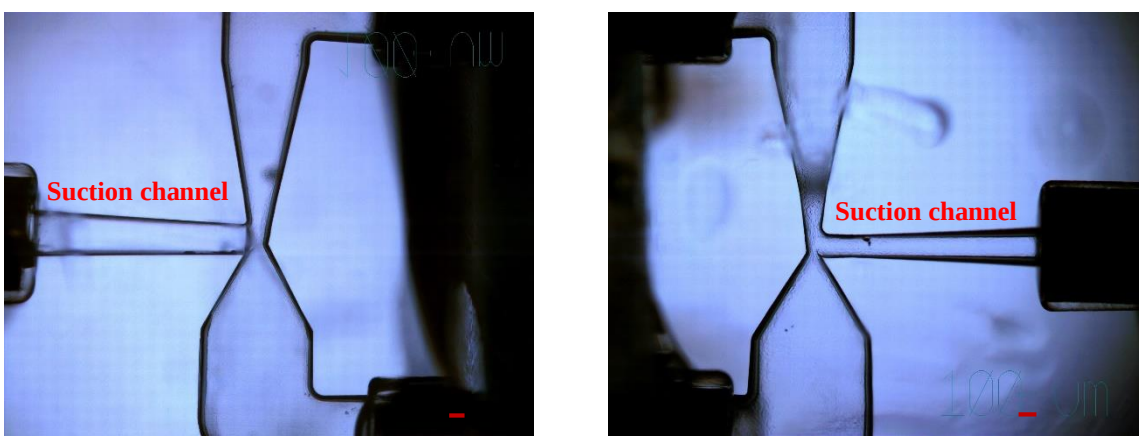

a) b)

Fig. 4 The micro-pump devices fabricated and etched in fused silica. (a) The second design approach with the ~ 100 µm wide vena contracta and the ~ 170 µm wide suction channel; (b) the third design approach with the ~ 62 µm wide vena contracta and the 122 µm wide suction channel.

The maximum suction effect was achieved when the vena contracta region was the narrowest. It is evident because the fluid speed was highest in the narrower channel. At the input and output part of the micro-channel, the wider channels of ~ 650 µm in diameter as connectors from micro to macro were fabricated. The sliced syringe needles were glued to the interconnectors with UV glue. Then the rubber hoses were connected and

glued to another needle side. The micro-pump device is shown in figure 5a. The inlet of the prepared device was connected to the internal micro diaphragm liquid pump (KNF N10) with the controlled flow rate. The suction pressure was measured with the vacuum sensor (SMC ZSE 30). The measured and simulated dependence of negative pressure on the input flow velocity is shown in figure 5 b.

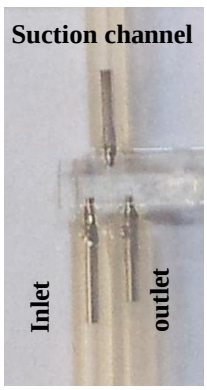

a)

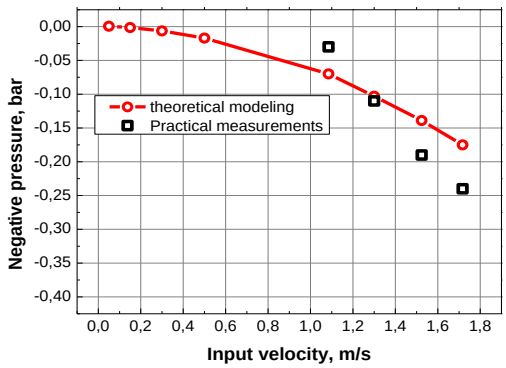

b)

Fig. 5 The fabricated micro-pump device (a) and the negative pressure dependence on the inlet fluid velocity (b).

The suction flow rate was measured by immersing the suction hose to the painted water cruet of a 2 ml volume. The suction time for 1 ml was measured, and according to this, the suction flow rate dependence on the inlet fluid velocity was estimated. The threshold inlet fluid velocity at which the fluid suction started in the suction channel was ~ 0.05 m/s for the micro-pump with the narrowest vena contracta (~62 µm). When the vena contracta size was increased, the threshold velocity increased. For the vena contracta of ~ 100 µm in size, it was ~ 0.4 m/s. The captured picture of working micro-pump is presented in figure 6.

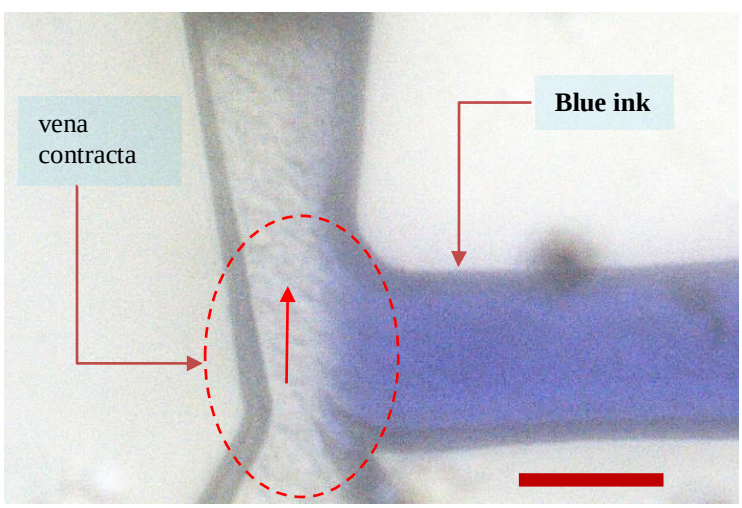

Fig 6 The captured with CCD camera working micro-pump device in the vena contracta region. The diluted blue ink was sucked in the suction channel and mixed with water. The red bar indicates 100 µm

4. Conclusion

The micro-pump device with mixing capability was demonstrated. The design of the device was optimized during the simulation. The inlet and outlet divergence angles have an influence on the suction capability. Several micro-pumps designs were simulated and fabricated. During the simulations, the optimized design of micro-pump was achieved by modelling different inlet and outlet divergence angles and also the width of the vena contracta region. Simulations showed that the optimal micro-pump design was when the inlet divergence angle was ~ 30 º, and outlet divergence angle was ~15 º. To achieve the significant negative pressure at the vena contracta, the ratio of the inlet to the vena contracta width should be large enough (> 6:1). Decreasing the width of the vena contracta, the threshold inlet velocity to achieve the suction reduces.

The femtosecond laser induced chemical etching technique has shown a flexible possibility to fabricate such type of micro devices.

5. References

Whitesides, G. M., 2006. The origins and the future of microfluidics, Nature, 442, p. 368.

Sackmann, E. K., Fulton, A. L., Beebe, D. J., 2014. The present and future role of microfluidics in biomedical research. Nature, 507, p. 181.

Pennathur S., 2008. Flow control in microfluidics: are the workhorse flows adequate? Lab Chip, 8, p. 383.

Zengerle R., Kluge S., Richter M., Richter A. 1995. A bidirectional silicon micropump. Microelectro-mechanical systems, MEMS'95, Proceedings. IEEE, p. 19.

Benard W. L., Kahn H, Heuer A. H.; Huff M. A., 1997. A titanium-nickel shape-memory-alloy actuated micropump. Proceedings of Transducers'97, p. 361.

Ahn C. H., Allen M.G., 1995. Fluid micropumps based on rotary magnetic actuator. Microelectro-mechanical systems, MEMS'95, Proceedings. IEEE p.408.

Manz A., Effenhauser C. S., Burggraf N., Harrison D. J., Seiler K. Flurri K., 1994. Electroosmotic pumping and electrophoretic separations for miniaturised chemical analysis systems, Journal of Micromechanics and Microengineering 4, p. 257.

Madou M. J., 2002. Fundamentals of microfabrication: the science of miniaturization. Naguib N. G. Raouf and Sherbet V. Gajann, Editor. CRC Press, Florida.

Hnatovsky C., Taylor R. S., Simova E., Rajeev P. P. Rajeev, Rayner D. M., Bhardwaj V. R., and Corkum P. B., 2006. Fabrication of microchannels in glass using focused femtosecond laser radiation and selective chemical etching. Applied. Physics A: Materials Science & Processing 84, p. 47.

Gattass R. R.; Mazur E., 2008. Femtosecond laser micromachining in transparent materials. Nature Photonics 2, p. 219.

Sugioka K., Cheng Y., 2014. Ultrafast lasers—reliable tools for advanced materials processing. Light Sci. Appl. 3, p. 149.

Bellouard Y., Said A., Dugan M. and Bado P., 2004. Fabrication of high-aspect ratio, micro-fluidic channels and tunnels using femtosecond laser pulses and chemical etching. Optics Express 12, p. 2120.

Marcinkevicius A., Juodkazis S., Watanabe M., Miwa M., Matsuo S., Misawa H. and Nishii J., 2001. Femtosecond laser-assisted three-dimensional microfabrication in silica. Opt. Lett. 26(5), 277–279 (2001).

laser-assisted three-dimensional microfabrication in silica," Optics Letters. 26, p. 277.

Koo K. I., Jeong M. J., Park S. K., Choi H. M., Kim K. S., Park J. H. and Cho D. I., 2006. Valveless, Venturi-tube Micro Suction Pump Using Solid Chemical Propellant.**,** World Congress, p. 306 Seoul, Korea.

Stankevič V., Račiukaitis G, 2014. Free-shape 3D Structure Formation in Bulk Fused Silica by Irradiation with Femtosecond Laser Pulses. Journal of Laser Micro/Nanoengineering, 9, p. 271.